



Cite this: *Phys. Chem. Chem. Phys.*,  
2018, 20, 17504

# Synthesis and photophysical properties of ruthenium(II) polyimine complexes decorated with flavin†

Huimin Guo,<sup>a</sup> Lijuan Zhu,<sup>a</sup> Can Dang,<sup>a</sup> Jianzhang Zhao<sup>a</sup> and Bernhard Dick<sup>b</sup>

A bipyridine ruthenium(II) complex (Ru-1) with a flavin moiety connected to one of the bipyridine ligands via an acetylene bond was designed and synthesized, and its photophysical properties were investigated. Compared with the tris(bipyridine) Ru(II) complex (Ru-0), which has an extinction coefficient  $\epsilon = 1.36 \times 10^4 \text{ M}^{-1} \text{ cm}^{-1}$  at 453 nm, the introduction of the flavin moiety endows Ru-1 with strong absorption in the visible range ( $\epsilon = 2.34 \times 10^4 \text{ M}^{-1} \text{ cm}^{-1}$  at 456 nm). Furthermore, Ru-1 exhibits phosphorescence ( $\lambda_{\text{em}} = 643 \text{ nm}$ ,  $\Phi_{\text{P}} = 1\%$ ,  $\tau_{\text{P}} = 1.32 \mu\text{s}$  at 293 K and  $4.53 \mu\text{s}$  at 77 K). We propose that the emission of Ru-1 originates from the low lying triplet excited state of  $^3\text{IL}$  according to the time-resolved transient difference absorption spectra, the calculated  $T_1$  spin density and the  $T_1$  thermo-vibration modes localized on the flavin-decorated bipyridine ligand. This is the first time that the phosphorescence of flavin was observed within Ru(II) complexes. Consequently, Ru-1 was used for triplet-triplet annihilation upconversion, showing a reasonable quantum yield of 0.7% with respect to the phosphorescence quantum yield of 1%. These findings pave the way for the rational design of phosphorescence transition metal complexes. Also, further approaches that may improve the performance of flavin-decorated Ru(II) bipyridine complexes are proposed.

Received 13th April 2018,  
Accepted 1st June 2018

DOI: 10.1039/c8cp02358a

rsc.li/pccp

## 1. Introduction

Recently, transition metal complexes such as those of Pt(II), Ir(III), and Ru(II) have received considerable attention due to their newly found applications in photocatalysis,<sup>1–5</sup> phosphorescent imaging and molecular sensing,<sup>6–13</sup> photodynamic therapy (PDT),<sup>14–16</sup> and triplet-triplet-annihilation based up-conversion (TTA UC),<sup>17–20</sup> where strong absorption in the visible range and a long-lived triplet excited state are crucial.<sup>21–23</sup> Different from conventional organic photosensitizers,<sup>24–27</sup> transition metal atoms with large atomic number can induce strong spin-orbital coupling (SOC) and facilitate the intersystem crossing (ISC) processes in these complexes, which are prohibited by selection rules. Due to this heavy atom effect, efficient ISCs and phosphorescence from the lowest triplet state ( $T_1$ ) are frequently observed in transition metal complexes.<sup>6,7,21–23</sup>

Although strong absorption in the visible light region is desirable for efficient energy conversion and electronic transfer to afford the expected excited states, the allowed ground state ( $S_0$ ) to singlet metal-ligand charge transfer state ( $^1\text{MLCT}$ ) transition in transitional metal complexes is commonly a weak absorption.<sup>28–31</sup> Furthermore, these complexes usually suffer from short  $T_1$  state lifetime, the elongation of which requires not only effective ISC mediated by the transition metal center to facilitate the formation of  $^3\text{MLCT}$ , but also the formation of equilibrium with or thermodynamically driving force for the transition from  $^3\text{MLCT}$  to triplet ligand localized excited state ( $^3\text{IL}$ ).<sup>21–23,32–35</sup> Consequently, the design of transition metal complexes for photosensitizer applications is challenging. Thus, a thorough understanding of the structure-properties correlation with the photophysical properties of these transition metal complexes is required to overcome the abovementioned challenges, which is currently unavailable.<sup>21–23,32–35</sup>

Ru(II) polypyridine complexes are representative transition metal complexes that show visible light absorption and can act as triplet photosensitizers, which have been used for solar energy harvesting, molecular sensors, molecular switches, etc.<sup>31,36</sup> The lowest singlet excited state of Ru(II) polypyridine complexes commonly shows  $^1\text{MLCT}$  character. After population at  $^1\text{MLCT}$ , the excited complex then relaxes to  $^3\text{MLCT}$  through ISC, which is

<sup>a</sup> State Key Laboratory of Fine Chemicals, School of Chemistry, Dalian University of Technology, Dalian, 116024, P. R. China. E-mail: guohm@dlut.edu.cn, zhaojzh@dlut.edu.cn

<sup>b</sup> Institut für Physikalische und Theoretische Chemie, Universität Regensburg, Regensburg, 93053, Germany

† Electronic supplementary information (ESI) available: The structural characterization spectra of FL, L-1, Ru-0 and Ru-1 and TD-DFT assignment of the absorption spectra. See DOI: 10.1039/c8cp02358a

facilitated by the Ru(II) center. The emission of Ru complexes is usually due to the radiative emission of  $^3\text{MLCT}$ , which is a broad, structureless band centered at  $\sim 600$  nm, with a luminescence lifetime usually less than  $1\ \mu\text{s}$ . The  $T_1$  lifetime may be extended further if the  $^3\text{MLCT}$  can evolve to or be in equilibrium with a  $^3\text{IL}$ , if such a state has a lower energy. Consequently, the triplet lifetime of  $T_1$  of these complexes are determined by the relative energy position of  $^3\text{MLCT}$ , a higher-lying metal centered triplet excited state ( $^3\text{MC}$ ) and the potential existence of  $^3\text{IL}$ .<sup>31</sup> With this insight, we successfully tailored the photophysical properties of Ru(II) polypyridine complexes, including both their absorption in visible light region and  $T_1$  lifetime, by incorporating organic chromophores in the polypyridine ligands, including coumarin,<sup>37–39</sup> pyrene,<sup>36,40</sup> rhodamine,<sup>41–43</sup> thiazole and benzothiazole,<sup>44</sup> benzotriazole,<sup>45</sup> carbazole,<sup>46</sup> and others.<sup>21–23</sup>

Flavin and its derivatives (FL) are structurally and functionally the reaction sites for redox-active coenzymes, which are capable of initiating a variety of thermal and photoinduced electron transfer processes over a wide range of redox potentials.<sup>47–53</sup> FL derivatives were found to act as electron acceptors in photoinduced electronic transfer to afford a long-lived charge separation state due to their small reorganization energies.<sup>52–55</sup> Furthermore, FL derivatives are known to bind various metal ions, which give rise to a positive shift in their one-electron reduction potentials.<sup>56,57</sup> Direct coordination of FL derivatives through their  $\text{N}^{\wedge}\text{N}$  or  $\text{N}^{\wedge}\text{O}$  to Ru(II), Co(II), Cu(II), Zn(II) and Cd(II) centers has been reported.<sup>58–65</sup> FL coordination to Ru(II) together with bipyridine ligands have been reported to afford Ru(II) complexes with  $T_1$  of  $^3\text{MC}$  character, in which the coordination of FL derivatives with Ru(II) is activated upon UV radiation, leading to isomerization of the complexes.<sup>58,59</sup> Due to the low reorganization energy of both FL derivatives and porphyrin, metalloporphyrin complexes of Sc(III), Zn(II) and Pd(II) decorated with FL derivatives were reported to exhibit elongated  $T_1$  lifetimes.<sup>66</sup> Although both FL derivatives and Ru(II) polypyridine complexes exhibit outstanding photophysical properties, to date, Ru(II) polypyridine complexes decorated with FL derivatives have not been reported, and the triplet emission of FL has not been observed within transition metal complexes.

In this study, we covalently attached FL to a bipyridine ligand to afford Ru-1 and investigated its photophysical properties by combining experimental and theoretical efforts. The covalent attachment of electron-acceptor moieties such as FL through an acetylene connection to the bipyridine ligand may enhance the conjugation within the ligand to afford strong absorption in the visible light region, avoid the competitive coordination of FL *via* N or O atoms to Ru(II), and help to facilitate the thermodynamically driven evolution of  $^3\text{MLCT}$  to  $^3\text{IL}$ .

## 2. Materials and methods

All chemicals used in the synthesis were analytically pure and used as received. Solvents were dried and distilled before

use for synthesis. All samples in the flash photolysis and upconversion experiments were deaerated with  $\text{N}_2$  for at least 15 min before measurement.

### Analytical measurements

All chemicals were analytically pure and used as received. NMR spectra were recorded on a Bruker 500 MHz spectrometer and OXFORD NMR 400 MHz spectrometer with  $\text{CDCl}_3$ ,  $\text{DMSO-d}_6$  or acetonitrile- $\text{d}_6$  as the solvent and tetramethylsilane (TMS) as the standard at 0.00 ppm. HRMS was accomplished with a MALDI micro MX (Waters, U.S.), GCT (Micromass, U.K.), G6224A (Agilent, U.S.) or LTQ Orbitrap XL (Thermo Scientific, U.S.). Fluorescence spectra were measured on an RF5301 PC spectrofluorometer (Shimadzu, Japan). Absorption spectra were recorded on a UV2550 UV-vis spectrophotometer (Shimadzu, Japan). Fluorescence lifetimes were measured with an OB920 luminescence lifetime spectrometer (Edinburgh, UK).

### Nanosecond transient absorption spectra

Nanosecond transient absorption spectra were measured on an LP980 laser flash photolysis spectrometer (Edinburgh Instruments, UK) and recorded on a Tektronix TDS 3012B oscilloscope and with a nanosecond pulsed laser (OpoletteTM 355II+UV nanosecond pulsed laser, typical pulse length: 7 ns; pulse repetition: 20 Hz; peak OPO energy: 6 mJ. The wavelength was tunable in the range of 200–2200 nm. OPOTEK, USA). The lifetime values (by monitoring the decay trace of the transients) were obtained with the LP900 software.

### Cyclic voltammetry

Cyclic voltammetry was performed at a scan rate of  $50\ \text{mV s}^{-1}$  on a CHI610D electrochemical workstation (Shanghai, China). The measurements were performed at room temperature with tetrabutylammonium hexafluorophosphate ( $\text{Bu}_4\text{N}[\text{PF}_6]$ , 0.1 M) as the supporting electrolyte, a glassy carbon electrode as the working electrode, and platinum electrode as the counter electrode. Acetonitrile was used as the solvent and ferrocene (Fc) was added as the internal reference. The solution was purged with  $\text{N}_2$  before the measurement, and the  $\text{N}_2$  gas flow was kept constant during the measurement.

### Triplet-triplet annihilation upconversion

A 473 nm cw-laser was used for the upconversion. The upconversion quantum yield ( $\Phi_{\text{UC}}$ ) was determined with the prompt fluorescence of  $[\text{Ru}(\text{bpy})_3]^{2+}$  ( $\Phi = 9.5\%$  in MeCN) as the standard. The upconversion quantum yield was calculated using eqn (1), where  $\Phi_{\text{UC}}$ ,  $A_{\text{sam}}$ ,  $I_{\text{sam}}$ , and  $\eta_{\text{sam}}$  represent the quantum yield, absorbance, integrated photoluminescence intensity, and refractive index of the sample, respectively. The corresponding terms for the subscript std are for the reference quantum counter. This equation was multiplied by a factor of 2 to set the maximum quantum yield to unity.

$$\Phi_{\text{UC}} = 2\Phi_{\text{std}} \left( \frac{1 - 10^{-A_{\text{std}}}}{1 - 10^{-A_{\text{sam}}}} \right) \left( \frac{I_{\text{sam}}}{I_{\text{std}}} \right) \left( \frac{\eta_{\text{sam}}}{\eta_{\text{std}}} \right)^2 \quad (1)$$

## Synthesis

The ligands and Ru(II) complexes were synthesized according to Scheme 1. The detailed synthesis conditions, yield, state of the compounds, yield and characterization are included in the (Section 2, ESI†).

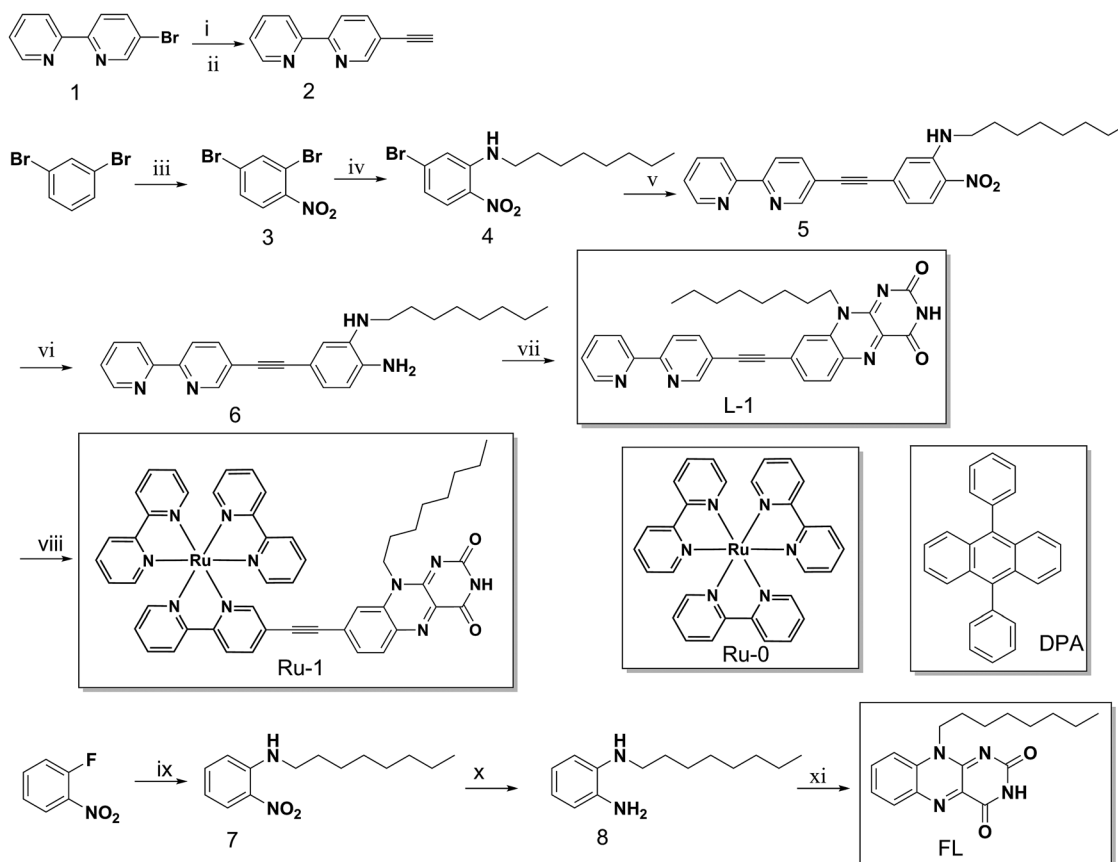
## Theoretical methods

Density functional theory (DFT) and time-dependent density functional theory (TD-DFT)-based calculations were performed to investigate the photophysical properties of the as-prepared compounds. The 6-31G(d) basis sets were used for the main group elements,<sup>67–69</sup> while the Los Alamos Effective Core Potentials (LanL2Dz) were used for Ru.<sup>70,71</sup> As the octyl group in the FL moiety is not involved in the photophysical process, it was replaced with a methyl group to lower the computational cost. The structures of the  $S_0$  states of the compounds were fully relaxed with the B3LYP functional.<sup>72,73</sup> Then, TD-DFT calculations at the same level of theory were performed to obtain the  $S_1$  and  $T_1$  structures. All these structures were verified with frequency calculations to be the local minima along the corresponding potential energy surface. All calculations were performed with Gaussian 09.<sup>74</sup> The transition dipole moments

from  $T_1$  to  $S_0$  were evaluated from the quadratic response function,<sup>75–77</sup> and the spin-orbit coupling matrix elements were computed at the same level of theory using the effective single-electron approximation in the linear response theory with Dalton.<sup>78–80</sup> The phosphorescent spectra of the Ru complexes were calculated using MOMAP.<sup>81–85</sup> Natural transition orbital (NTO) analysis was performed to understand the electron transitions involved in the UV-vis absorption using Multiwfn and Gaussian 09.<sup>74,86</sup> The polarizable continuum model (PCM) was applied to take into account the electrostatic interaction with the solvent.<sup>87–89</sup> These methods were previously used to investigate the photophysics of organic dyes and Ir(III) complexes, and the obtained results were in excellent agreement with the experiments.<sup>90,91</sup>

## 3. Results and discussions

Inspired by our previous studies reporting that  $^3\text{IL}$  emission can be observed *via* the decoration of bipyridine ligands attached to a Ru(II) center with organic chromophores, we used FL to decorate the bipyridine ligand to tailor the photophysical properties of the Ru(II) bipyridine complex. The synthesis routes and



**Scheme 1** Synthesis of the compounds. (i) Trimethylsilylacetylene,  $\text{Pd}(\text{PPh}_3)_2\text{Cl}_2$ ,  $\text{PPh}_3$ ,  $\text{CuI}$ ,  $\text{Et}_3\text{N}$ , reflux, 8 h. Yield: 66.2%. (ii)  $\text{Bu}_4\text{NF}$ , THF, r.t. Yield: 58.2%. (iii) Concentrated sulphuric acid, concentrated nitric acid, r.t., 2 h. Yield: 73.8%. (iv) *N*-Octylamine,  $\text{Et}_3\text{N}$ , THF, reflux, 15 h. Yield: 98.7%. (v)  $\text{Pd}(\text{PPh}_3)_4$ ,  $\text{CuI}$ ,  $\text{Et}_3\text{N}$ , reflux, 8 h. Yield: 71%. (vi) Zinc, ammonium chloride, methanol,  $\text{H}_2\text{O}$ , reflux, 3 h. (vii) Alloxan, boric acid, acetic acid glacial, 60 °C, 1 h. Yield: 33.7%. (viii)  $[\text{RuCl}_2(\text{cymene})]_2$ , 2,2'-dipyridyl, ethanol,  $\text{H}_2\text{O}$ . Yield: 15%; (ix) *N*-octylamine,  $\text{Et}_3\text{N}$ , THF, reflux, 9 h. Yield: 98.5%. (x) Zinc, ammonium chloride, methanol,  $\text{H}_2\text{O}$ . Yield: 95%. (xi) Alloxan, boric acid, acetic acid glacial, 60 °C, 1 h. Yield: 41%.

compounds involved in this investigation are shown in Scheme 1. FL (FL, Scheme 1) was attached to the bipyridine ligand *via* an acetylene group to afford the FL decorated bipyridine ligand (L-1, Scheme 1), which was used to afford complex Ru-1 (Ru-1, Scheme 1). All the Ru(II) complexes, FL and ligands used in this study were prepared in accordance with standard procedures with final purification and are readily soluble in a variety of organic solvents. All the compounds were obtained with good yields and were structurally characterized *via* NMR and mass spectrometry (see Section 2 and ESI† for details). The structures and properties of FL, L-1 and the previously reported compound Ru-0 were also characterized to investigate the photophysical properties of Ru-1.<sup>37,40</sup>

The UV/vis absorption spectra of FL, L-1 and Ru-1 in dichloromethane (DCM) are shown in Fig. 1a. The UV/vis spectrum of FL is characterized by two absorption bands at  $\sim 350$  and  $\sim 450$  nm, which is in good agreement with the reported results.<sup>92,93</sup> The UV/vis absorption spectra of L-1 and FL are similar, which have 2 absorption bands with maxima in the range of 300–400 nm and 400–500 nm, respectively. The conjugation with the acetylene bonds and the bipyridine ligands further red-shifts these bands and enhances their intensity with respect to FL. The strong absorption of L-1 and FL in the visible light range is characterized by their molar extinction coefficients ( $\epsilon$ ) of  $1.10 \times 10^4$  and  $1.95 \times 10^4$  M<sup>-1</sup> cm<sup>-1</sup>, respectively. The similarity in their absorption implies that FL and L-1 exhibit similar photophysical properties under UV radiation. Ru-1 shows the most intense absorption in the range of 240–500 nm and its calculated  $\epsilon$  is  $2.34 \times 10^4$  M<sup>-1</sup> cm<sup>-1</sup>. This is almost double that of Ru-0 with  $\epsilon$  of  $1.36 \times 10^4$  M<sup>-1</sup> cm<sup>-1</sup> and more than twice that of FL. These results are in reasonable agreement with those obtained for Ru(II) bipyridine complexes decorated with coumarin and pyrene, which demonstrates the feasibility of our approach.<sup>36,37,40</sup> Furthermore, the strong absorption feature of L-1 in the visible range can be recognized in Ru-1. Thus, the strong absorption of Ru-1 can be attributed to L-1, which is in accord with the TD-DFT calculations (Table 1 and Fig. 2).

We then investigated the absorption of Ru-1 in toluene, DCM, acetonitrile and methanol (Fig. 1b). The <sup>1</sup>MLCT absorption band of Ru-0 at  $\sim 450$  nm was proposed to be charge-transfer in nature, which may lead to the formation of a dipolar

excited state, and is thus sensitive to the polarity of the solvent.<sup>94</sup> This will be further enhanced as the FL in L-1 alters its symmetry and polarity with respect to Ru-0. Thus, DFT/TD-DFT calculations were performed to understand the absorption spectra of Ru-1. All the electronic transitions with excitation wavelength above 350 nm including the dark states not mentioned in Table 1 are shown in Table S1 (ESI†), and the orbitals involved in these transitions are shown in Fig. S36 (ESI†). To justify the accuracy of the calculation,<sup>95</sup> DFT/TD-DFT calculations with the PBE0 functional and 6-31g(d,p)//LanL2dz basis sets were also performed, which yielded principally the same physical picture for the absorption (Table S2 and Fig. S37, ESI†). Additionally, NTO analysis was performed for electronic transitions with oscillator strength larger than 0.2 to uncover the nature of the transitions (Table S3 and Fig. S38, ESI†). Our TD/DFT calculations interpreted that the absorption at  $\sim 450$  nm ( $S_0 \rightarrow S_4$ ) is contributed by both the LLCT within L-1 and MLCT from Ru(II) to L-1. This confirms the contribution of L-1 to the enhanced absorption in this region and also the MLCT nature of the transition. Since the introduction of the FL moiety in L-1 extends the conjugation and differentiates the energy levels of L-1 and bipyridine ligands, the absorption at  $\sim 406$  nm ( $S_0 \rightarrow S_{11}$ ) is attributed to MLCT from the Ru-d states to FL and bipyridine moiety of L-1 and LLCT between L-1 and bipyridine ligands. Additionally, the absorption at  $\sim 396$  nm ( $S_0 \rightarrow S_{13}$ ) can be attributed to the MLCT from Ru-d to the bipyridine ligands and LLCT between L-1 and the bipyridine ligands (Table S3 and Fig. S38, ESI†). Moreover, the photophysics of FL is quite complex. FL possesses abundant alkyl O, pyridinic N and imidic N within a  $\pi$ -conjugated planar framework, which are available for formation of  $\pi$ - $\pi$  stacking, hydrogen bonds and electron transfer with the solvent. Therefore, its absorption is very sensitive to the environment and is solvent-dependent.<sup>50</sup> As an overall effect, the absorption of Ru-1 is solvent dependent and its arbitrary absorption intensity in DCM was slightly higher than in the other solvents investigated.<sup>94</sup>

A similar solvent dependent phenomenon was also observed for the emission spectra of the ligands and Ru(II) complexes. The emission spectra of FL and L-1 (Fig. 3a and b) share the same character, with emission bands at  $\sim 500$  and  $\sim 510$  nm, respectively. The vibrational structures of FL and L-1 are

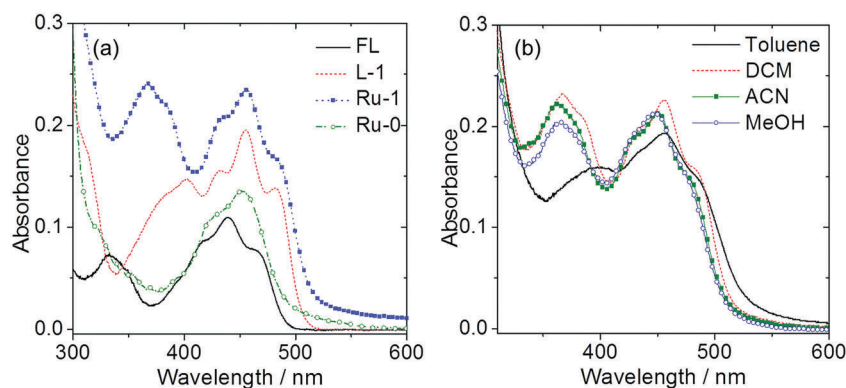


Fig. 1 (a) UV-vis absorption spectra of FL, L-1, Ru-0 and Ru-1 in DCM. (b) UV-vis absorption spectra of Ru-1 in different solvents.  $c = 1.0 \times 10^{-5}$  M; 293 K.

**Table 1** Major electronic transitions involved in the excitation of Ru-1. (Please see Table S1 (ESI) for a full analysis of the electronic transitions within visible light region including the dark states.)<sup>a</sup>

Electronic transitions	Energy	$f^b$	Composition <sup>c</sup>	CI <sup>d</sup>	Character
$S_0 \rightarrow S_1$	2.32 eV/533 nm	0.0189	194 $\rightarrow$ 195	0.64339	M $\rightarrow$ L', L $\rightarrow$ L'
			194 $\rightarrow$ 196	0.26961	M $\rightarrow$ L', L $\rightarrow$ L'
$S_0 \rightarrow S_2$	2.51 eV/494 nm	0.0341	192 $\rightarrow$ 195	0.19016	M $\rightarrow$ L', L $\rightarrow$ L'
			193 $\rightarrow$ 195	0.62141	M $\rightarrow$ L', L $\rightarrow$ L'
			193 $\rightarrow$ 196	0.24274	d $\rightarrow$ d, L $\rightarrow$ L'
$S_0 \rightarrow S_3$	2.57 eV/482 nm	0.0435	191 $\rightarrow$ 195	0.12279	L $\rightarrow$ L', M $\rightarrow$ L'
			192 $\rightarrow$ 195	0.62775	M $\rightarrow$ L', L $\rightarrow$ L'
			192 $\rightarrow$ 196	0.19108	d $\rightarrow$ d, L $\rightarrow$ L'
			193 $\rightarrow$ 195	0.20520	M $\rightarrow$ L', L $\rightarrow$ L'
$S_0 \rightarrow S_4$	2.73 eV/455 nm	1.0202	191 $\rightarrow$ 195	0.67220	L $\rightarrow$ L', M $\rightarrow$ L'
			192 $\rightarrow$ 195	0.14582	L $\rightarrow$ L', M $\rightarrow$ L'
$S_0 \rightarrow S_{11}$	3.06 eV/406 nm	0.2304	190 $\rightarrow$ 195	0.51368	L $\rightarrow$ L', M $\rightarrow$ L'
			192 $\rightarrow$ 195	0.10233	L $\rightarrow$ L', M $\rightarrow$ L'
			192 $\rightarrow$ 196	0.20748	d $\rightarrow$ d, L $\rightarrow$ L'
			193 $\rightarrow$ 195	0.10656	L $\rightarrow$ L', M $\rightarrow$ L'
			193 $\rightarrow$ 196	0.27452	d $\rightarrow$ d, L $\rightarrow$ L'
$S_0 \rightarrow S_{13}$	3.13 eV/396 nm	0.3002	193 $\rightarrow$ 198	0.25900	d $\rightarrow$ d, L $\rightarrow$ L'
			190 $\rightarrow$ 195	0.42016	L $\rightarrow$ L', M $\rightarrow$ L'
			192 $\rightarrow$ 195	0.11688	L $\rightarrow$ L', M $\rightarrow$ L'
			192 $\rightarrow$ 196	0.43253	d $\rightarrow$ d, L $\rightarrow$ L'
			192 $\rightarrow$ 198	0.13864	d $\rightarrow$ d, L $\rightarrow$ L'
$S_0 \rightarrow T_1$	1.91 eV/648 nm		193 $\rightarrow$ 196	0.11101	d $\rightarrow$ d, L $\rightarrow$ L'
			193 $\rightarrow$ 198	0.24588	d $\rightarrow$ d, L $\rightarrow$ L'
			191 $\rightarrow$ 195	0.18128	L $\rightarrow$ L', M $\rightarrow$ L'
			192 $\rightarrow$ 195	0.14374	L $\rightarrow$ L', M $\rightarrow$ L'
			193 $\rightarrow$ 195	0.55639	L $\rightarrow$ L', M $\rightarrow$ L'
$S_0 \rightarrow T_2$	2.22 eV/558 nm		193 $\rightarrow$ 196	0.12541	d $\rightarrow$ d, L $\rightarrow$ L'
			194 $\rightarrow$ 195	0.26434	L $\rightarrow$ L', M $\rightarrow$ L'
			190 $\rightarrow$ 195	0.41180	L $\rightarrow$ L', M $\rightarrow$ L'
			191 $\rightarrow$ 195	0.20563	L $\rightarrow$ L', M $\rightarrow$ L'
			193 $\rightarrow$ 195	0.13039	L $\rightarrow$ L', M $\rightarrow$ L'
$S_0 \rightarrow T_3$	2.40 eV/517 nm		193 $\rightarrow$ 196	0.16664	d $\rightarrow$ d, L $\rightarrow$ L'
			194 $\rightarrow$ 195	0.33718	L $\rightarrow$ L', M $\rightarrow$ L'
			194 $\rightarrow$ 196	0.23733	L $\rightarrow$ L', M $\rightarrow$ L'
			194 $\rightarrow$ 197	0.15482	d $\rightarrow$ d, L $\rightarrow$ L'
			190 $\rightarrow$ 195	0.38775	L $\rightarrow$ L', M $\rightarrow$ L'
			191 $\rightarrow$ 195	0.12892	L $\rightarrow$ L', M $\rightarrow$ L'
			193 $\rightarrow$ 195	0.16429	L $\rightarrow$ L', M $\rightarrow$ L'
			193 $\rightarrow$ 196	0.13207	d $\rightarrow$ d, L $\rightarrow$ L'
			194 $\rightarrow$ 195	0.40457	L $\rightarrow$ L', M $\rightarrow$ L'
			194 $\rightarrow$ 196	0.18273	L $\rightarrow$ L', M $\rightarrow$ L'
			194 $\rightarrow$ 197	0.16080	d $\rightarrow$ d, L $\rightarrow$ L'

<sup>a</sup> For  $S_0 \rightarrow S_n$  transitions, only the first 4 and the major transitions with an oscillator strength larger than 0.2 are shown. The first 3  $S_0 \rightarrow T_n$  transitions are also shown. <sup>b</sup> Oscillator strength, not available for  $S_0 \rightarrow T_n$  transitions. <sup>c</sup> Only the main configurations are presented. <sup>d</sup> The CI coefficients are in absolute values.

observable in toluene and DCM and their emission intensities decrease in high polarity methanol and acetonitrile due to the high polarity of the solvents and the vibrational decay of their  $S_1$  states. The emission of Ru(II) bipyridine complexes from their low lying  $^3\text{MLCT}$  states has been widely accepted due to the heavy atom effect of Ru(II).<sup>31</sup> Since Ru-0 emits from  $^3\text{MLCT}$ , which is an excited state with its charge transfer populated by ISC from  $^1\text{MLCT}$  and  $\lambda_{\text{em}}$  of 595 nm, the observed phosphorescence is more sensitive to the polarity of the solvent (Fig. 3c). The measured phosphorescence lifetime of Ru-1 in a mixture of

ethanol/methanol is 0.58  $\mu\text{s}$  at 293 K and 4.9  $\mu\text{s}$  at 77 K, which is typical for the emission of Ru(II) complexes.<sup>96</sup> The phosphorescence emission behavior of Ru-1 (Fig. 3d) was further identified because it can be quenched by  $\text{O}_2$ , while the  $^3\text{IL}$  nature of the lowest triplet state of Ru-1 was suggested by the TDDFT/DFT calculated energy levels and compositions of the low lying triplet excited states (Table 1, Fig. 2 and Table S4, Fig. S39, ESI<sup>†</sup>), excited state spin charge density localized at L-1 (Fig. 4), and the emission of Ru-1 centered at  $\sim 650$  nm with a lifetime of 1.32  $\mu\text{s}$  (Fig. 3).



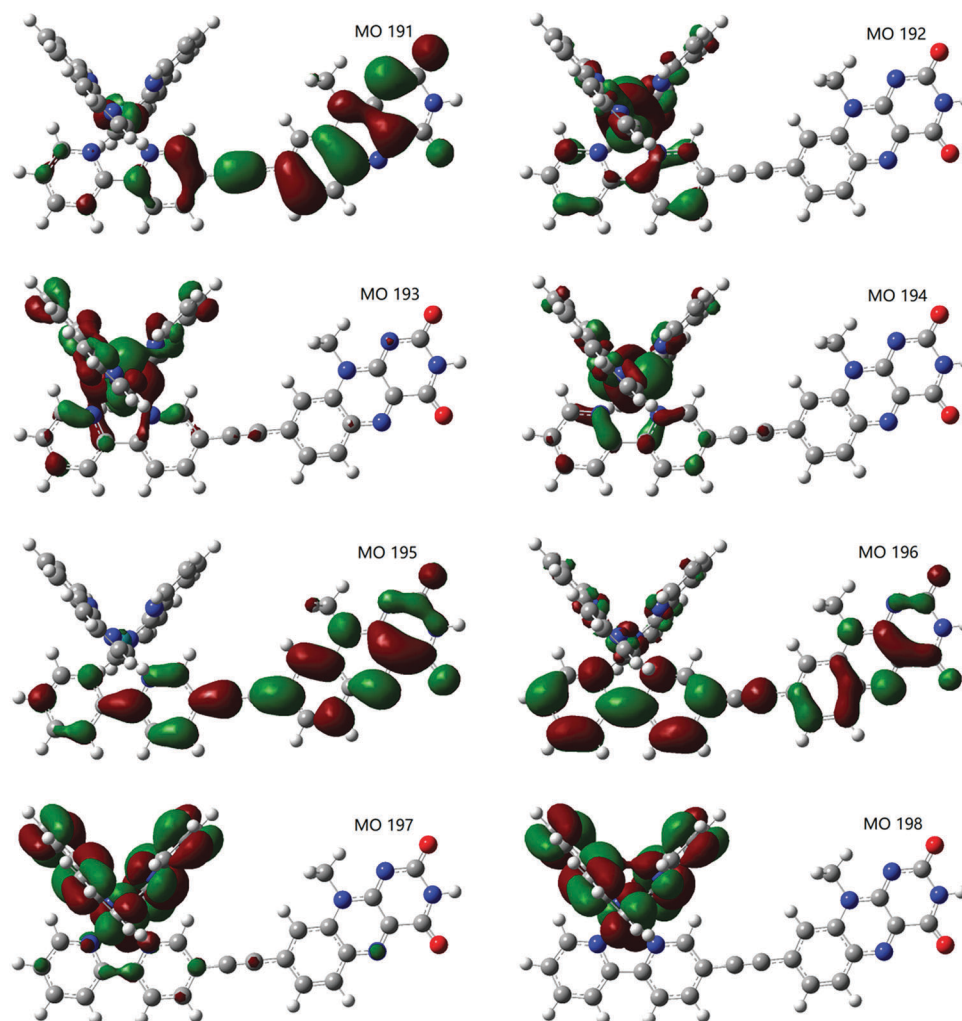


Fig. 2 Contour plots of the wavefunction of the molecular states of Ru-1 involved in the transitions mentioned in Table 1. The Ru, C, O, N, and H atoms are in cyan, gray, red, blue and white, respectively. The isovalue is  $\pm 0.02$  a.u. Please see Fig. S36 (ESI<sup>†</sup>) for a full version of the wavefunctions involved in the electronic transitions within the visible light region.

In Ru-1, L-1 completely breaks the symmetry around the octahedral Ru(II) center, making the emission from  $T_1$  of Ru-1 too sensitive to the solvent; thus, its emission is only observable in DCM (Fig. 3d). We noticed that the measured phosphorescence lifetime of Ru-0 is slightly longer than that of Ru-1 ( $4.90 \mu\text{s}$  vs.  $4.53 \mu\text{s}$  in DCM at 77 K). This is due to the fact that Ru(II) not only facilitates ISC from  $^1\text{MLCT}$  to  $^3\text{MLCT}$ , which further evolves to  $^3\text{IL}$  delocalized on L-1, but also promotes the feasibility of ISC from  $^3\text{IL}$  to  $S_0$ .<sup>92</sup> Furthermore, the complex photophysics of the flavin moiety that makes the emission and absorption of FL moiety sensitive to the environment may also play a role in the emission.<sup>50</sup> Since the emission of Ru-1 is only significant in DCM, the emission of FL, L-1, Ru-1 and Ru-0 were further investigated in DCM at 293 K at a concentration of  $1 \times 10^{-5}$  M. By fitting the decay trace, the emission lifetimes of FL, L-1 and Ru-1 were determined to be 6.53 ns, 1.65 ns and 1.32  $\mu\text{s}$ , respectively. These results further confirm that the emission of FL and L-1 is of fluorescent in nature, while that of Ru-1 is phosphorescent.

Electrochemical characterization was also performed to address the proposed charge transfer nature of the solvent dependent absorption and emission of FL, L-1, Ru-1 and Ru-0. In brief, only one reversible reduction wave was observed for Ru-1 at  $-0.68$  V and corresponding reduction waves were observed in FL, EFL and L-1 at  $-1.09$ ,  $-0.93$  and  $-0.83$  V, respectively. Therefore, the reversible reduction wave for Ru-1 is contributed by the FL moiety within Ru-1. However, for Ru-0, three reduction waves were observed at  $-1.73$ ,  $-1.92$  and  $-2.17$  V, all of which are attributed to the Ru(II) coordination center. Furthermore, the oxidation waves of Ru-0 and Ru-1 were observed at  $+0.90$  and  $+0.93$  V, respectively. We then calculated the Gibbs free energy change ( $\Delta G_{\text{es}}$ ) of the electron transfer process using the Rehm–Weller equation to enhance the understanding of the photo-induced electron transfer (PET) in Ru-1. It was found that PET in polar solvents such as acetonitrile is exothermic ( $\Delta G_{\text{es}} = -0.41$  eV). However, in less polar solvents such as DCM  $\Delta G_{\text{es}}$  is  $-0.23$  eV; hence, PET is partially inhibited due to the small exothermic nature of the process with the lack of driving force.

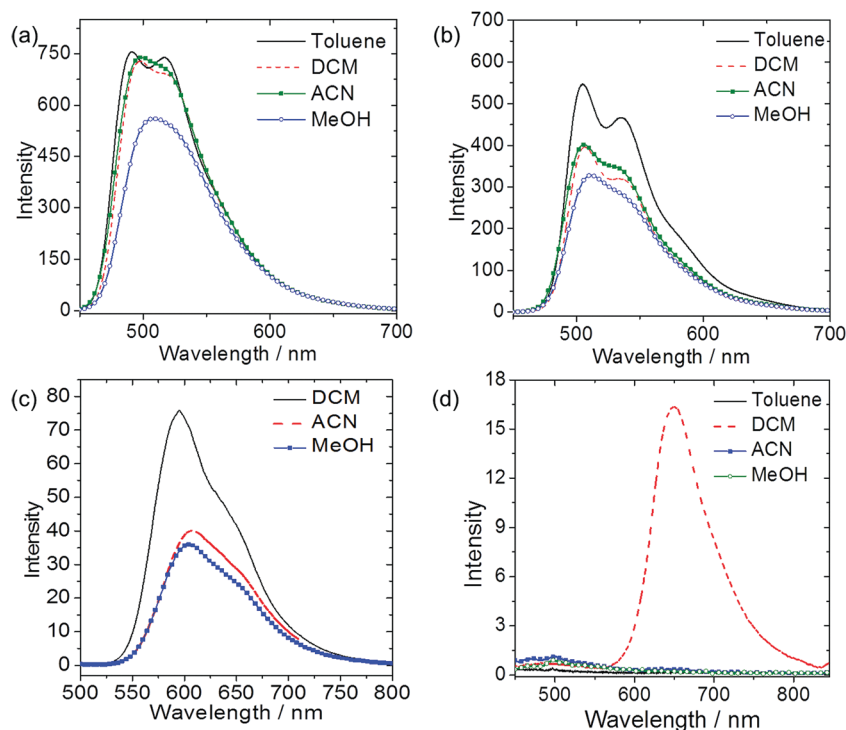


Fig. 3 Emission spectra of the ligands FL (a) and L-1 (b) and complexes Ru-0 (c) and Ru-1 (d) in different solvents.  $c = 1.0 \times 10^{-5}$  M; 293 K.

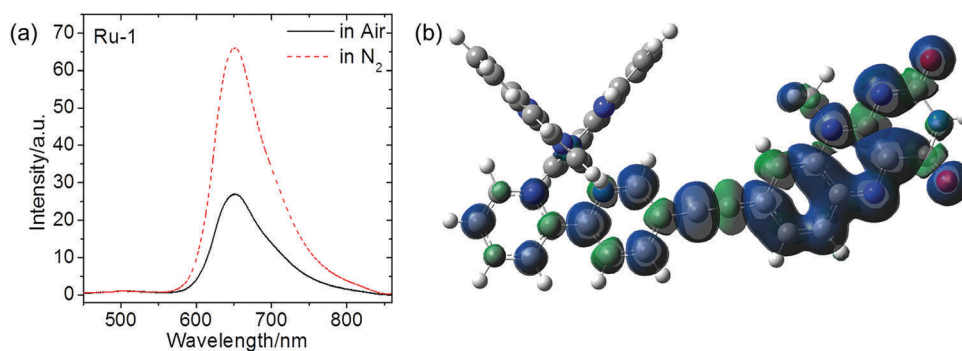


Fig. 4 (a) Emission spectra of Ru-1 in DCM saturated with air and  $N_2$  ( $\lambda_{em} = 651$  nm,  $c = 1.0 \times 10^{-5}$  M; 293 K). (b) Contour plot of the TDDFT/DFT calculated  $T_1$  spin density of Ru-1 (isovalue = 0.0004 a.u., Ru, C, O, N, and H atoms are in cyan, gray, red, blue and white, respectively).

This further explains the observed emission of Ru-1 in DCM (Fig. 3d). We also calculated the energy levels for the charge transfer states (CTS). In acetonitrile,  $E_{CTS}$  is 1.58 eV, which is lower than the energy of the lowest lying triplet state of Ru-1 (Table 1,  $T_1$ ). Therefore, the phosphorescence of Ru-1 is completely quenched by PET in acetonitrile (Fig. 3d). However, the  $E_{CTS}$  in DCM is higher than the energy of the lowest lying triplet state of Ru-1; thus, the emission of Ru-1 is observable. In the case of toluene, the weak emission is due to the formation of  $\pi$ - $\pi$  stacking. These results, to some extent, further explain the solvent dependent nature of the absorption and emission of Ru-1 and support the aforementioned proposal for the emission from  $^3IL$  of Ru-1.

We also noticed that the emission of Ru-1 is strong in nitrogen saturated solution (Fig. 4a), but is partially quenched

under air atmosphere or in oxygen saturated solution (not shown). The sensitivity of the emission to  $O_2$  provides evidence that Ru-1 emits from its low lying triplet excited states and the phosphorescence emission of Ru-1 is sensitive to  $O_2$ . However, the emission under air atmosphere is still observable compared to that under  $N_2$  atmosphere as a result of the efficient ISC from the proposed  $S_1$  to  $T_1$ . According to our previous experience on the  $O_2$  sensing behavior of Ru(II) bipyridine complexes, these results suggest the potential  $O_2$  sensing application of Ru-1 if its phosphorescence lifetime can be further elongated by molecular design.<sup>36,37,40</sup>

The emissions of FL, L-1, Ru-0 and Ru-1 at 77 K and 293 K were also compared in Fig. 5. The emission of FL, L-1 and Ru-0 were measured in ethanol/methanol mixture, while that of Ru-1 was measured in DCM. The vibrational fine structures of all

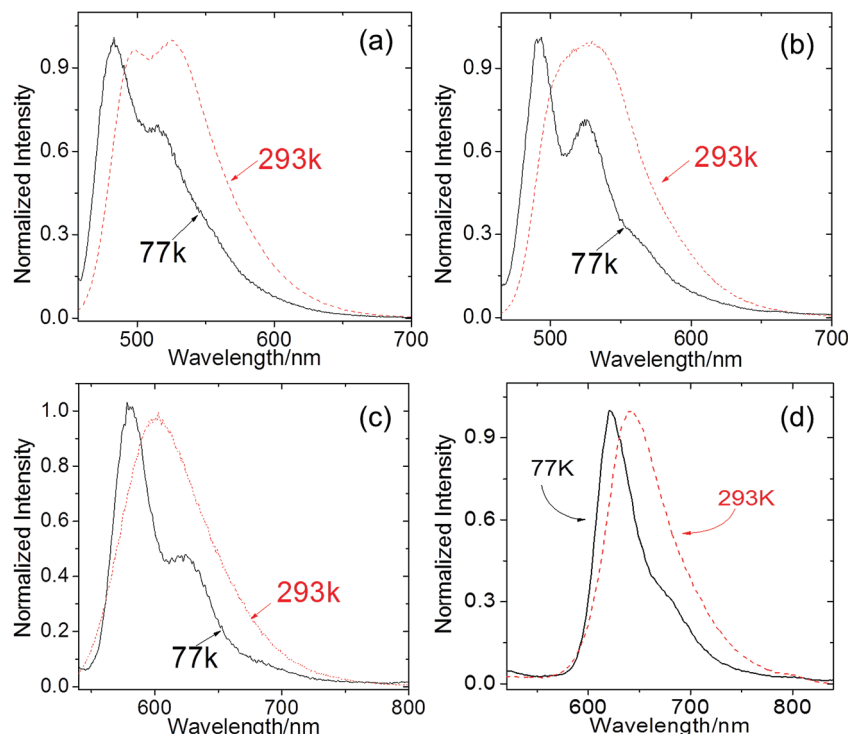


Fig. 5 Normalized emission spectra of (a) FL, (b) L1, and (c) Ru-0 ( $\lambda_{\text{ex}} = 445$  nm) in ethanol-methanol (4:1, v/v) glass at 77 K and at 293 K under a deaerated atmosphere. (d) Emission spectra of Ru-1 in  $\text{CH}_2\text{Cl}_2$  under an atmosphere of  $\text{N}_2$  at 77 K and at 293 K.

these compounds were observed at 77 K. The emissions of FL and L-1 are quite similar, which demonstrates that their emission originates from the  $\text{S}_1$  state on the FL moiety. At 77 K, two emission bands centered at  $\sim 495$  and  $\sim 520$  nm are observed for FL and L-1, which overlap into one peak at 293 K. Ru-0 and Ru-1 also demonstrate significant vibrational progression at 77 K. The thermal induced Stokes shift of Ru-0 is slightly more significant than that of Ru-1 (23 nm vs. 18 nm). It has been accepted that a small thermal-induced Stokes shift is established evidence for the  $^3\text{IL}$  components in the low lying triplet excited states corresponding to the emission.<sup>97,98</sup> Previously, the emission of Ru-0 was proposed to be  $^3\text{MLCT}$ , but the small thermal-induced Stokes shift of 18 nm suggests that the emission of Ru-1 has greater  $^3\text{IL}$  component.<sup>37,40</sup> This is in good accordance with the aforementioned calculated  $\text{T}_1$  spin density localized on L-1. The decay traces of Ru-1 were fitted to a first-order decay function and the obtained phosphorescence lifetimes at 77 K and 293 K are 4.53 and 1.32  $\mu\text{s}$ , respectively. Since the inter-molecular collision and vibration along non-emissive decay paths are diminished to a large extent at lower temperatures, the obtained phosphorescence lifetime at 77 K is much longer than that at 293 K.

We then used nanosecond time-resolved transient absorption spectra to probe the emission nature of FL, L-1, Ru-1 and Ru-0 (Fig. 6). The transient absorption spectrum of FL is characterized by ground-state bleach at 442 nm and excited state absorption at 372 and in the range of 500–700 nm, corresponding to FL triplet absorption (Fig. 6a).<sup>92</sup> Similar to FL, the peaks for the ground-state bleach of L-1 are located at 375 and 460 nm, while that for

the triplet excited states absorption are red shifted to the range above 500 nm and below 300 nm due to the delocalization within the L-1 ligand (Fig. 6b). The excited state absorption above 500 nm is due to the triplet lifetime of FL.<sup>92,99</sup> The measured L-1 triplet lifetime of 27.3  $\mu\text{s}$  is also typical for FL derivatives.<sup>99–102</sup> In the case of Ru-1, the major peak for ground state bleach is at 365 nm and there are 2 minor bleaching peaks at 432 and 453 nm, which is in good accordance with its strong absorption in the visible light range (Fig. 1a). The significant triplet excited state absorption falls in the range below 300 nm (not shown) and 478–750 nm. The transient absorption behavior of Ru-1 is completely different to that of Ru-0, where the transient absorption typical for  $^3\text{MLCT}$  is located at  $\sim 320$  nm and no triplet absorption peak is found from 500 to 700 nm (Fig. 6d). According to the transient absorption behavior of FL, L-1 and Ru-1, their excited state absorption in the range of 478–750 nm can be attributed to formation of  $^3\text{IL}$  state delocalized on L-1 of Ru-1 (Fig. 6b). Previously, similar triplet excited state absorptions in the range of 600–700 nm were reported for an FL mononucleotide and I-substituted FL using transient absorption spectroscopy,<sup>92,101</sup> which are in reasonable agreement with our findings. The triplet lifetime of Ru-1 of 0.62  $\mu\text{s}$  was then determined by fitting the decay trace at 651 nm. Since the concentration of Ru-1 is higher ( $3.0 \times 10^{-5}$  M) in the transient absorption experiments than that used to characterize the emission spectra, the shortened triplet lifetime can be attributed to the enhanced inter-molecular collision and vibration along non-emissive decay pathways. To the best of our knowledge, this is the first time that triplet emission of FL derivatives is observed in an Ru(II) complex.



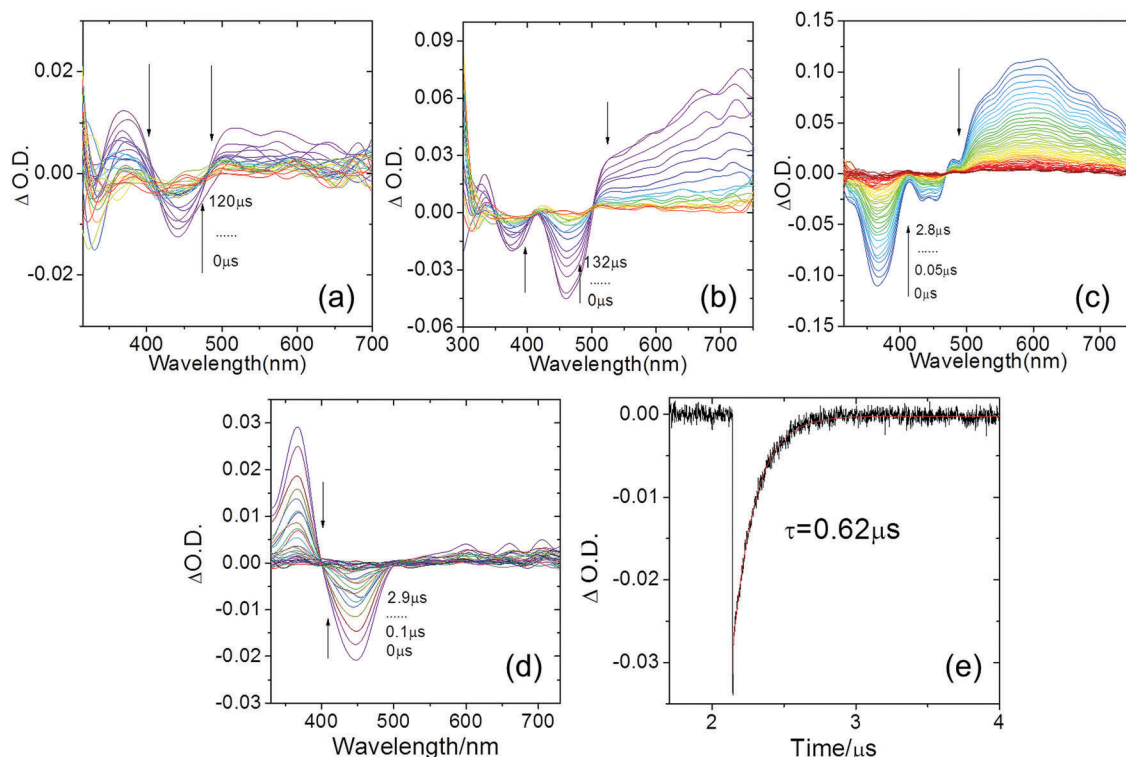


Fig. 6 Nanosecond time-resolved transient absorption spectra. (a) FL ( $\lambda_{\text{ex}} = 430$  nm); (b) L-1 ( $\lambda_{\text{ex}} = 445$  nm); (c) Ru-1 ( $\lambda_{\text{ex}} = 447$  nm); and (d) Ru-0 ( $\lambda_{\text{ex}} = 441$  nm). (e) Decay trace of Ru-1 at 650 nm after pulsed laser excitation ( $\lambda_{\text{ex}} = 447$  nm).  $c = 3.0 \times 10^{-5}$  M in deaerated  $\text{CH}_2\text{Cl}_2$ ; 293 K.

The photophysical parameters of these compounds are summarized in Table 2. According to its high triplet yield, L-1 is a potential catalyst for the oxidation of benzoic alcohols.<sup>103</sup> Furthermore, Ru-1 exhibits the properties of enhanced absorption in the visible range and a reasonable triplet lifetime. Consequently, it can, in principle, be used as a photosensitizer to initiate photophysical processes that need a triplet excited state. In a practical attempt, Ru-1 was used as a photosensitizer for triplet-triplet annihilation-based upconversion. The emissions of Ru-1 in the presence and absence of DPA (Scheme 1) are shown in Fig. 7a. In the presence of DPA, upconverted fluorescence in the range 400–500 nm was observed upon the selective radiation of sensitizers at 473 nm. Irradiation of DPA alone did not produce any emission, and thus proves the role of Ru-1 as a triplet sensitizer. The peak area of the quenched

phosphorescence emission of Ru-1 by DPA is not significant, although the upconverted fluorescence is significant. The determined upconversion quantum yield was 0.7%. We propose that a non-emissive portion of the Ru-1 sensitizer in the triplet state is involved because the phosphorescence emission of Ru-1 is relatively weak with a quantum yield of only 1%.

The Stern-Volmer plot of Ru-1 is shown in Fig. 7b and a photo of the TTA UC is shown in Fig. 7c. The calculated Stern-Volmer quenching constant ( $K_{\text{sv}}$ ) is  $5.80 \times 10^3 \text{ M}^{-1}$  and the bimolecular quenching constant ( $k_q$ ) is  $4.39 \times 10^9 \text{ M}^{-1} \text{ s}^{-1}$ , which are comparable to that of Ru-0.<sup>37</sup> This is the first time that an Ru(II) complex derived from FL is used for upconversion applications. We propose that the reasonable upconversion performance of Ru-1 is due to its special structural feature introduced by the FL moiety, as already exemplified by its triplet lifetime.

Table 2 Photophysical parameters of the studied compounds

	$\lambda_{\text{abs}}^a/\text{nm}$	$\epsilon^b$	$\lambda_{\text{em}}^c/\text{nm}$	$\Phi_{\text{F}}$	$\tau_{\text{T}}^f/\mu\text{s}$	$\Phi_{\Delta}^g$	$\Phi_{\text{T}}^h$	$\tau_{\text{F}}/\text{ns}$
FL	438	0.110	507; 536	0.363 <sup>d</sup>	37.8	0.427	0.279	5.97; <sup>i</sup> 6.09; <sup>j</sup> 7.94 <sup>k</sup>
L-1	455	0.195	508; 537	0.192 <sup>d</sup>	27.3	0.488	0.769	1.80; <sup>i</sup> 1.83; <sup>j</sup> 2.72 <sup>k</sup>
Ru-1	456	0.234	643	0.010 <sup>e</sup>	0.62	0.274	0.244	1.32 $\mu\text{s}$ ; <sup>n</sup> 4.53 $\mu\text{s}$ <sup>o</sup>
Ru-0	453	0.136	595	0.095 <sup>m</sup>	0.45	0.57 <sup>m</sup>	1.000 <sup>m</sup>	0.27 $\mu\text{s}$ ; <sup>i</sup> 0.58 $\mu\text{s}$ ; <sup>l</sup> 4.9 $\mu\text{s}$ <sup>k</sup>

<sup>a</sup> In  $\text{CH}_2\text{Cl}_2$  ( $c = 1.0 \times 10^{-5}$  M). <sup>b</sup> Molar absorption coefficient.  $\epsilon$ :  $10^5 \text{ M}^{-1} \text{ cm}^{-1}$ . <sup>c</sup> Maximum emission wavelength in  $\text{CH}_2\text{Cl}_2$  ( $1.0 \times 10^{-5}$  M). <sup>d</sup> The fluorescence quantum yields with perylene ( $\Phi_{\text{F}} = 98\%$ , in hexane) as the standard. <sup>e</sup> The phosphorescence quantum yields with  $\text{Ru}(\text{bpy})_3^{2+}$  ( $\Phi_{\text{p}} = 9.5\%$ , in deaerated MeCN) as the standard under  $\text{N}_2$ . <sup>f</sup> Measured by transient absorption in toluene ( $3.0 \times 10^{-5}$  M). <sup>g</sup> Singlet oxygen quantum yields in  $\text{CH}_2\text{Cl}_2$ ;  $\text{Ru}(\text{bpy})_3^{2+}$  was used as the standard ( $\Phi_{\Delta} = 0.57$  in MeCN). <sup>h</sup> Triplet quantum yields in  $\text{CH}_2\text{Cl}_2$ .  $\text{Ru}(\text{bpy})_3^{2+}$  was used as the standard ( $\Phi_{\text{T}} = 1.00$  in MeCN). <sup>i</sup> At 293 K, measured in air in MeOH–EtOH solvent. <sup>j</sup> At 293 K, measured in deaerated MeOH–EtOH solvent. <sup>k</sup> At 77 K, EtOH/MeOH = 4/1 (v/v) ( $1.0 \times 10^{-5}$  M). <sup>l</sup> Measured in deaerated solution ( $\text{N}_2$ ). <sup>m</sup> Literature values. <sup>n</sup> At 293 K, measured in deaerated  $\text{CH}_2\text{Cl}_2$ . <sup>o</sup> At 77 K, measured in  $\text{CH}_2\text{Cl}_2$ .

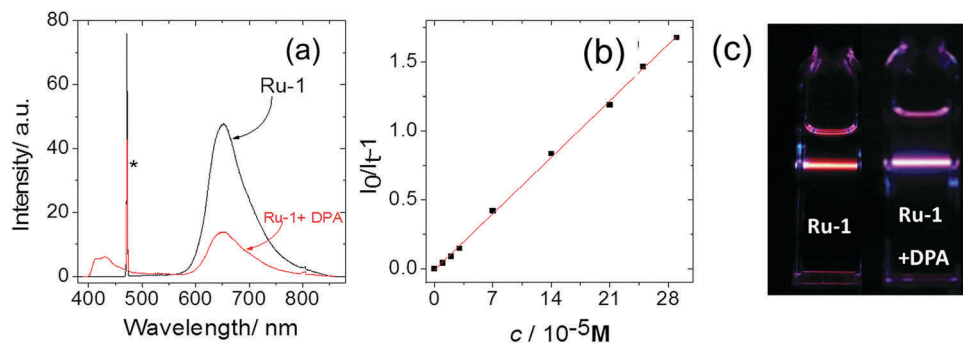


**Fig. 7** Upconversion with Ru-1 as the triplet photosensitizer and DPA as the triplet acceptor. (a) Excited by 473 nm laser (5.2 mW). The asterisks indicate the scattered laser.  $c(\text{sensitizers}) = 1.0 \times 10^{-5} \text{ M}$  and  $c(\text{DPA}) = 4.2 \times 10^{-4} \text{ M}$ , in deaerated  $\text{CH}_2\text{Cl}_2$ , 293 K. (b) Stern–Volmer plots generated from the intensity-quenching of the Ru-1 complex. DPA as a quencher.  $c(\text{photosensitizers}) = 1.0 \times 10^{-5} \text{ M}$ ,  $\lambda_{\text{ex}} = 473 \text{ nm}$  in  $\text{CH}_2\text{Cl}_2$ , 293 K. (c) Photograph of TTA UC.

Considering these results, we resorted to the vibration resolved emission spectrum to back up our proposal for the  $^3\text{IL}$  nature of the lowest lying triplet excited state and the potential ways to strengthen the emission properties of Ru-1. The TDDFT/DFT simulated phosphorescent emission of Ru-1 takes place with the first maximum at  $\sim 700 \text{ nm}$ , which is in reasonable agreement with the experimental  $\lambda_{\text{em}}$  of 651 nm (Fig. 8a). The reorganization

energy corresponding to the non-emissive structure transition along the normal modes on the  $\text{S}_0$  energy surface from the  $\text{T}_1$  structure was then projected onto the  $\text{S}_0$  normal modes according to the calculated Huang factors in Fig. 8b. The reorganization energy was found to be contributed mainly by the normal modes 66, 163, 204, 205 and 207. These modes were reprojected back to the vibration resolved phosphorescence spectrum of

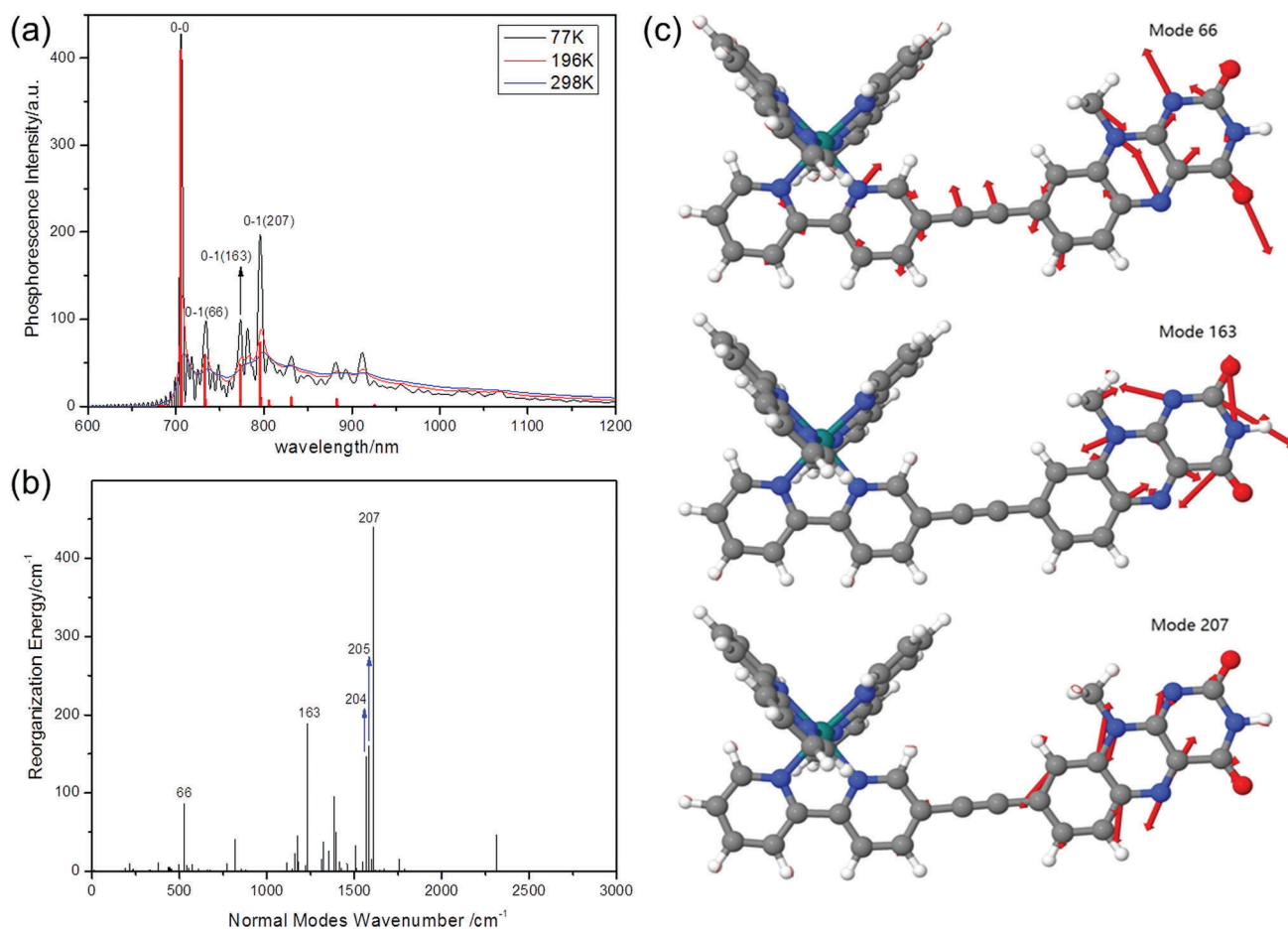


**Fig. 8** Simulated phosphorescent spectra at 77, 198 and 298 K (a). Projection of reorganization energy into the vibrational normal modes on the  $\text{S}_0$  surface (b). Corresponding vibration modes (c).

Ru-1 (Fig. 8a). The thermo-reorganization that competes with the phosphorescent emission is mainly contributed by normal modes, namely, 0-1(66), 0-1(163) and 0-1(207). Only the C and N atoms within the FL moiety are involved in these normal modes. The atomic motions corresponding to these modes were then analyzed, as shown in Fig. 8c. It can be observed that 0-1(66) is the in-plane asymmetric motion of N atoms within L-1, and 0-1(164) and 0-1(207) are contributed by the stretching of (C=N)-C(=O) within the FL moiety. These findings further strengthen our proposal of the important role of FL in the phosphorescent emission within Ru-1. Accordingly, the vibrations within the FL moiety are the main processes that compete with the phosphorescent emission within Ru-1. Thus, to diminish these non-emissive energy consumption pathways, the FL moiety should be more closely connected to the Ru(II) center to maintain efficient ISC, while FL should be further modified to be more rigid to achieve prolonged triplet lifetime by extending the conjugated framework within L-1 to lower its contribution to the reorganization energies, particularly those along the C-N direction.

## 4. Conclusions

A bipyridine ruthenium(II) complex (Ru-1) with a flavin moiety connected to one of the bipyridine ligands via an acetylene bond was designed and synthesized and its photophysical properties were carefully characterized. The triplet state emission of the flavin chromophore was identified through nanosecond time-resolved transient difference absorption spectra and TDDFT/DFT calculations. The room temperature phosphorescence of the flavin moiety was observed ( $\lambda_{\text{em}} = 651$  nm,  $\Phi_{\text{P}} = 1\%$ , and  $\tau_{\text{T}} = 2.83$   $\mu\text{s}$ ) within Ru-1 for the first time. The comparison with the alternative complex Ru-0, which has  $\varepsilon = 1.36 \times 10^4$   $\text{M}^{-1} \text{cm}^{-1}$  at 453 nm, revealed that Ru-1 also shows strong absorption in the visible range ( $\varepsilon = 2.35 \times 10^4$   $\text{M}^{-1} \text{cm}^{-1}$  at 456 nm). The emissive triplet excited state of Ru-1 was characterized as  $^3\text{IL}$ . The complex was used for TTA UC, showing a reasonable upconversion quantum yield of 0.7% with respect to the phosphorescence quantum yield of 1%. These findings pave the way for the rational design of phosphorescent transition metal complexes with strong absorption in the visible light region. Further studies are being carried out to improve the  $^3\text{IL}$  emission behavior of bipyridine Ru(II) complexes for applications in processes where a triplet sensitizer is vital, such as photooxidation.

## Author contributions

H. M. Guo designed this research after discussion with B. Dick and J. Z. Zhao and wrote the manuscript. L. J. Zhu performed the experimental research with the guidance of H. M. Guo and J. Z. Zhao. C. Dang performed the theoretical calculations with the guidance of H. M. Guo. L. J. Zhu and C. Dang are responsible for the results presented. The manuscript was written through contributions of all authors. H. M. Guo finalized the manuscript.

## Conflicts of interest

There are no conflicts to declare.

## Acknowledgements

This study was supported by National Natural Science Foundation of China (NSFC, No. 21573034, 21771029, 21373036 and 21103015). The supercomputer time was provided by National Supercomputing Center in Guangzhou, China and the High Performance Computing Center at Dalian University of Technology.

## References

- 1 R. R. Islangulov, D. V. Kozlov and F. N. Castellano, *Chem. Commun.*, 2005, 3776–3778.
- 2 O. S. Wenger, *Chem. – Eur. J.*, 2011, **17**, 11692–11702.
- 3 S. Jasimuddin, T. Yamada, K. Fukujū, J. Otsuki and K. Sakai, *Chem. Commun.*, 2010, **46**, 8466–8468.
- 4 J. F. Dong, M. Wang, P. Zhang, S. Q. Yang, J. Y. Liu, X. Q. Li and L. C. Sun, *J. Phys. Chem. C*, 2011, **115**, 15089–15096.
- 5 F. Gartner, S. Denurra, S. Losse, A. Neubauer, A. Boddien, A. Gopinathan, A. Spannenberg, H. Junge, S. Lochbrunner, M. Blug, S. Hoch, J. Busse, S. Gladiali and M. Beller, *Chem. – Eur. J.*, 2012, **18**, 3220–3225.
- 6 Q. A. Zhao, F. Y. Li and C. H. Huang, *Chem. Soc. Rev.*, 2010, **39**, 3007–3030.
- 7 V. Fernandez-Moreira, F. L. Thorp-Greenwood and M. P. Coogan, *Chem. Commun.*, 2010, **46**, 186–202.
- 8 E. Baggeley, J. A. Weinstein and J. A. G. Williams, *Coord. Chem. Rev.*, 2012, **256**, 1762–1785.
- 9 R. B. P. Elmes, M. Erby, S. A. Bright, D. C. Williams and T. Gunnlaugsson, *Chem. Commun.*, 2012, **48**, 2588–2590.
- 10 K. K. W. Lo, A. W. T. Choi and W. H. T. Law, *Dalton Trans.*, 2012, **41**, 6021–6047.
- 11 K. K. W. Lo and T. K. M. Lee, *Inorg. Chem.*, 2004, **43**, 5275–5282.
- 12 K. K. W. Lo, T. K. M. Lee, J. S. Y. Lau, W. L. Poon and S. H. Cheng, *Inorg. Chem.*, 2008, **47**, 200–208.
- 13 K. K. W. Lo, T. K. M. Lee and K. Y. Zhang, *Inorg. Chim. Acta*, 2006, **359**, 1845–1854.
- 14 A. Gorman, J. Killoran, C. O'Shea, T. Kenna, W. M. Gallagher and D. F. O'Shea, *J. Am. Chem. Soc.*, 2004, **126**, 10619–10631.
- 15 S. O. McDonnell, M. J. Hall, L. T. Allen, A. Byrne, W. M. Gallagher and D. F. O'Shea, *J. Am. Chem. Soc.*, 2005, **127**, 16360–16361.
- 16 W. T. Wu, X. D. Shao, J. Z. Zhao and M. B. Wu, *Adv. Sci.*, 2017, **4**, 1700113.
- 17 T. N. Singh-Rachford and F. N. Castellano, *Coord. Chem. Rev.*, 2010, **254**, 2560–2573.
- 18 P. Ceroni, *Chem. – Eur. J.*, 2011, **17**, 9560–9564.
- 19 A. Monguzzi, R. Tubino, S. Hoseinkhani, M. Campione and F. Meinardi, *Phys. Chem. Chem. Phys.*, 2012, **14**, 4322–4332.
- 20 Y. C. Simon and C. Weder, *J. Mater. Chem.*, 2012, **22**, 20817–20830.

- 21 J. Z. Zhao, S. M. Ji and H. M. Guo, *RSC Adv.*, 2011, **1**, 937–950.
- 22 J. Z. Zhao, S. M. Ji, W. H. Wu, W. T. Wu, H. M. Guo, J. F. Sun, H. Y. Sun, Y. F. Liu, Q. T. Li and L. Huang, *RSC Adv.*, 2012, **2**, 1712–1728.
- 23 J. Z. Zhao, W. H. Wu, J. F. Sun and S. Guo, *Chem. Soc. Rev.*, 2013, **42**, 5323–5351.
- 24 M. Kasha, *Chem. Rev.*, 1947, **41**, 401–419.
- 25 S. K. Lower and M. A. Elsayed, *Chem. Rev.*, 1966, **66**, 199–241.
- 26 H. Levanon and J. R. Norris, *Chem. Rev.*, 1978, **78**, 185–198.
- 27 M. C. Cuquerella, V. Lhiaubet-Vallet, J. Cadet and M. A. Miranda, *Acc. Chem. Res.*, 2012, **45**, 1558–1570.
- 28 V. Wing-Wah Yam and E. Chung-Chin Cheng, in *Photochemistry and Photophysics of Coordination Compounds II*, ed. V. Balzani and S. Campagna, Springer Berlin Heidelberg, Berlin, Heidelberg, 2007, DOI: 10.1007/128\_2007\_127, pp. 269–309.
- 29 L. Flamigni, A. Barbieri, C. Sabatini, B. Ventura and F. Barigelletti, in *Photochemistry and Photophysics of Coordination Compounds II*, ed. V. Balzani and S. Campagna, Springer Berlin Heidelberg, Berlin, Heidelberg, 2007, DOI: 10.1007/128\_2007\_131, pp. 143–203.
- 30 J. A. G. Williams, in *Photochemistry and Photophysics of Coordination Compounds II*, ed. V. Balzani and S. Campagna, Springer Berlin Heidelberg, Berlin, Heidelberg, 2007, , DOI: 10.1007/128\_2007\_134, pp. 205–268.
- 31 S. Campagna, F. Puntoriero, F. Nastasi, G. Bergamini and V. Balzani, in *Photochemistry and Photophysics of Coordination Compounds I*, ed. V. Balzani and S. Campagna, Springer Berlin Heidelberg, Berlin, Heidelberg, 2007, DOI: 10.1007/128\_2007\_133, pp. 117–214.
- 32 J. Z. Zhao, K. J. Xu, W. B. Yang, Z. J. Wang and F. F. Zhong, *Chem. Soc. Rev.*, 2015, **44**, 8904–8939.
- 33 P. T. Chou, Y. Chi, M. W. Chung and C. C. Lin, *Coord. Chem. Rev.*, 2011, **255**, 2653–2665.
- 34 N. Armaroli, *ChemPhysChem*, 2008, **9**, 371–373.
- 35 N. D. McClenaghan, Y. Leydet, B. Maubert, M. T. Indelli and S. Campagna, *Coord. Chem. Rev.*, 2005, **249**, 1336–1350.
- 36 S. M. Ji, W. H. Wu, W. T. Wu, P. Song, K. L. Han, Z. G. Wang, S. S. Liu, H. M. Guo and J. Z. Zhao, *J. Mater. Chem.*, 2010, **20**, 1953–1963.
- 37 S. M. Ji, H. M. Guo, W. T. Wu, W. H. Wu and J. Z. Zhao, *Angew. Chem., Int. Ed.*, 2011, **50**, 8283–8286.
- 38 W. H. Wu, S. M. Ji, W. T. Wu, J. Y. Shao, H. M. Guo, T. D. James and J. Z. Zhao, *Chem. – Eur. J.*, 2012, **18**, 4953–4964.
- 39 R. Nomula, X. Y. Wu, J. Z. Zhao and N. R. Munirathnam, *Mater. Sci. Eng., C*, 2017, **79**, 710–719.
- 40 S. M. Ji, W. H. Wu, W. T. Wu, H. M. Guo and J. Z. Zhao, *Angew. Chem., Int. Ed.*, 2011, **50**, 1626–1629.
- 41 X. N. Cui, J. Z. Zhao, A. Karatay, H. G. Yaglioglu, M. Hayvali and B. Kucukoz, *Eur. J. Inorg. Chem.*, 2016, 5078.
- 42 J. S. Wang, Y. Lu, N. McGoldrick, C. S. Zhang, W. B. Yang, J. Z. Zhao and S. M. Draper, *J. Mater. Chem. C*, 2016, **4**, 6131–6139.
- 43 W. H. Wu, J. F. Sun, X. N. Cui and J. Z. Zhao, *J. Mater. Chem. C*, 2013, **1**, 4577–4589.
- 44 C. H. Siu, C. L. Ho, J. He, T. Chen, X. N. Cui, J. Z. Zhao and W. Y. Wong, *J. Organomet. Chem.*, 2013, **748**, 75–83.
- 45 K. J. Xu, J. Z. Zhao and E. G. Moore, *Photochem. Photobiol. Sci.*, 2016, **15**, 995–1005.
- 46 C. H. Siu, C. L. Ho, J. He, T. Chen, P. Majumda, J. Z. Zhao, H. Li and W. Y. Wong, *Polyhedron*, 2014, **82**, 71–79.
- 47 C. Walsh, *Acc. Chem. Res.*, 1980, **13**, 148–155.
- 48 C. Walsh, *Acc. Chem. Res.*, 1986, **19**, 216–221.
- 49 T. C. Bruice, *Acc. Chem. Res.*, 1980, **13**, 256–262.
- 50 P. F. Heelis, *Chem. Soc. Rev.*, 1982, **11**, 15–39.
- 51 P. F. Heelis, R. F. Hartman and S. D. Rose, *Chem. Soc. Rev.*, 1995, **24**, 289–297.
- 52 W. Kaim and B. Schwederski, *Pure Appl. Chem.*, 2004, **76**, 351–364.
- 53 W. Kaim, B. Schwederski, O. Heilmann and F. M. Hornung, *Coord. Chem. Rev.*, 1999, **182**, 323–342.
- 54 M. Murakami, K. Ohkubo and S. Fukuzumi, *Chem. – Eur. J.*, 2010, **16**, 7820–7832.
- 55 W. Kaim and B. Schwederski, *Coord. Chem. Rev.*, 2010, **254**, 1580–1588.
- 56 S. Fukuzumi and K. Ohkubo, *Coord. Chem. Rev.*, 2010, **254**, 372–385.
- 57 M. B. Twitchett, J. C. Ferrer, P. Siddarth and A. G. Mauk, *J. Am. Chem. Soc.*, 1997, **119**, 435–436.
- 58 S. Miyazaki, T. Kojima and S. Fukuzumi, *J. Am. Chem. Soc.*, 2008, **130**, 1556–1557.
- 59 S. Miyazaki, K. Ohkubo, T. Kojima and S. Fukuzumi, *Angew. Chem., Int. Ed.*, 2007, **46**, 905–908.
- 60 E. R. Acuna-Cueva, R. Faure, N. A. Illan-Cabeza, S. Jimenez-Pulido, M. N. Moreno-Carretero and M. Quiros-Olozabal, *Inorg. Chim. Acta*, 2003, **342**, 209–218.
- 61 D. Das, T. K. Mondal, A. D. Chowdhury, F. Weisser, D. Schweinfurth, B. Sarkar, S. M. Mobin, F. A. Urbanos, R. Jimenez-Aparicio and G. K. Lahiri, *Dalton Trans.*, 2011, **40**, 8377–8390.
- 62 D. Maity, C. Bhaumik, D. Mondal and S. Baitalik, *Inorg. Chem.*, 2013, **52**, 13941–13955.
- 63 P. Mondal, R. Ray, A. Das and G. K. Lahiri, *Inorg. Chem.*, 2015, **54**, 3012–3021.
- 64 M. Subat, A. S. Borovik and B. Konig, *J. Am. Chem. Soc.*, 2004, **126**, 3185–3190.
- 65 P. Nieto, A. Gunther, G. Berden, J. Oomens and O. Dopfer, *J. Phys. Chem. A*, 2016, **120**, 8297–8308.
- 66 T. Kojima, R. Kobayashi, T. Ishizuka, S. Yamakawa, H. Kotani, T. Nakanishi, K. Ohkubo, Y. Shiota, K. Yoshizawa and S. Fukuzumi, *Chem. – Eur. J.*, 2014, **20**, 15518–15532.
- 67 R. C. Binning and L. A. Curtiss, *J. Comput. Chem.*, 1990, **11**, 1206–1216.
- 68 M. M. Francl, W. J. Pietro, W. J. Hehre, J. S. Binkley, M. S. Gordon, D. J. Defrees and J. A. Pople, *J. Chem. Phys.*, 1982, **77**, 3654–3665.
- 69 V. A. Rassolov, M. A. Ratner, J. A. Pople, P. C. Redfern and L. A. Curtiss, *J. Comput. Chem.*, 2001, **22**, 976–984.
- 70 P. J. Hay and W. R. Wadt, *J. Chem. Phys.*, 1985, **82**, 270–283.
- 71 W. R. Wadt and P. J. Hay, *J. Chem. Phys.*, 1985, **82**, 284–298.
- 72 A. D. Becke, *J. Chem. Phys.*, 1993, **98**, 5648–5652.



- 73 C. T. Lee, W. T. Yang and R. G. Parr, *Phys. Rev. B: Condens. Matter Mater. Phys.*, 1988, **37**, 785–789.
- 74 M. J. Frisch, G. W. Trucks, H. B. Schlegel, G. E. Scuseria, M. A. Robb, J. R. Cheeseman, G. Scalmani, V. Barone, G. A. Petersson, H. Nakatsuji, X. Li, M. Caricato, A. V. Marenich, J. Bloino, B. G. Janesko, R. Gomperts, B. Mennucci, H. P. Hratchian, J. V. Ortiz, A. F. Izmaylov, J. L. Sonnenberg, D. Williams-Young, F. Ding, F. Lipparini, F. Egidi, J. Goings, B. Peng, A. Petrone, T. Henderson, D. Ranasinghe, V. G. Zakrzewski, J. Gao, N. Rega, G. Zheng, W. Liang, M. Hada, M. Ehara, K. Toyota, R. Fukuda, J. Hasegawa, M. Ishida, T. Nakajima, Y. Honda, O. Kitao, H. Nakai, T. Vreven, K. Throssell, J. A. Montgomery Jr., J. E. Peralta, F. Ogliaro, M. J. Bearpark, J. J. Heyd, E. N. Brothers, K. N. Kudin, V. N. Staroverov, T. A. Keith, R. Kobayashi, J. Normand, K. Raghavachari, A. P. Rendell, J. C. Burant, S. S. Iyengar, J. Tomasi, M. Cossi, J. M. Millam, M. Klene, C. Adamo, R. Cammi, J. W. Ochterski, R. L. Martin, K. Morokuma, O. Farkas, J. B. Foresman and D. J. Fox, *Gaussian 09, Revision D01*, 2016.
- 75 O. Vahtras, H. Agren, P. Jorgensen, H. J. A. Jensen, T. Helgaker and J. Olsen, *J. Chem. Phys.*, 1992, **97**, 9178–9187.
- 76 H. Hettema, H. J. A. Jensen, P. Jorgensen and J. Olsen, *J. Chem. Phys.*, 1992, **97**, 1174–1190.
- 77 H. Agren, O. Vahtras, H. Koch, P. Jorgensen and T. Helgaker, *J. Chem. Phys.*, 1993, **98**, 6417–6423.
- 78 J. Olsen, D. L. Yeager and P. Jorgensen, *J. Chem. Phys.*, 1989, **91**, 381–388.
- 79 P. Jorgensen, H. J. A. Jensen and J. Olsen, *J. Chem. Phys.*, 1988, **89**, 3654–3661.
- 80 K. Aidas, C. Angeli, K. L. Bak, V. Bakken, R. Bast, L. Boman, O. Christiansen, R. Cimiraglia, S. Coriani, P. Dahle, E. K. Dalskov, U. Ekstrom, T. Enevoldsen, J. J. Eriksen, P. Ettenhuber, B. Fernandez, L. Ferrighi, H. Fliegl, L. Frediani, K. Hald, A. Halkier, C. Hattig, H. Heiberg, T. Helgaker, A. C. Hennum, H. Hettema, E. Hjertenaes, S. Host, I. M. Hoyvik, M. F. Iozzi, B. Jansik, H. J. A. Jensen, D. Jonsson, P. Jorgensen, J. Kauczor, S. Kirpekar, T. Kjrgaard, W. Klopper, S. Knecht, R. Kobayashi, H. Koch, J. Kongsted, A. Krapp, K. Kristensen, A. Ligabue, O. B. Lutnaes, J. I. Melo, K. V. Mikkelsen, R. H. Myhre, C. Neiss, C. B. Nielsen, P. Norman, J. Olsen, J. M. H. Olsen, A. Osted, M. J. Packer, F. Pawlowski, T. B. Pedersen, P. F. Provasi, S. Reine, Z. Rinkevicius, T. A. Ruden, K. Ruud, V. V. Rybkin, P. Salek, C. C. M. Samson, A. S. de Meras, T. Saue, S. P. A. Sauer, B. Schimmelpfennig, K. Sneskov, A. H. Steindal, K. O. Sylvester-Hvid, P. R. Taylor, A. M. Teale, E. I. Tellgren, D. P. Tew, A. J. Thorvaldsen, L. Thogersen, O. Vahtras, M. A. Watson, D. J. D. Wilson, M. Ziolkowski and H. Agren, *Wiley Interdiscip. Rev.: Comput. Mol. Sci.*, 2014, **4**, 269–284.
- 81 Q. Peng, Y. P. Yi, Z. G. Shuai and J. S. Shao, *J. Chem. Phys.*, 2007, **126**, 114302.
- 82 Q. Peng, Y. P. Yi, Z. G. Shuai and J. S. Shao, *J. Am. Chem. Soc.*, 2007, **129**, 9333–9339.
- 83 Y. L. Niu, Q. A. Peng, C. M. Deng, X. Gao and Z. G. Shuai, *J. Phys. Chem. A*, 2010, **114**, 7817–7831.
- 84 Y. Niu, Q. Peng and Z. Shuai, *Sci. China, Ser. B: Chem.*, 2008, **51**, 1153–1158.
- 85 Q. Peng, Y. L. Niu, Q. H. Shi, X. Gao and Z. G. Shuai, *J. Chem. Theory Comput.*, 2013, **9**, 1132–1143.
- 86 T. Lu and F. W. Chen, *J. Comput. Chem.*, 2012, **33**, 580–592.
- 87 S. Miertsus, E. Scrocco and J. Tomasi, *Chem. Phys.*, 1981, **55**, 117–129.
- 88 R. Cammi and B. Mennucci, *J. Chem. Phys.*, 1999, **110**, 9877–9886.
- 89 J. Tomasi, B. Mennucci and R. Cammi, *Chem. Rev.*, 2005, **105**, 2999–3093.
- 90 X. Zhang, D. Jacquemin, Q. Peng, Z. G. Shuai and D. Escudero, *J. Phys. Chem. C*, 2018, **122**, 6340–6347.
- 91 Q. Peng, Q. H. Shi, Y. L. Niu, Y. P. Yi, S. R. Sun, W. Q. Li and Z. G. Shuai, *J. Mater. Chem. C*, 2016, **4**, 6829–6838.
- 92 K. A. Korvinson, G. N. Hargenrader, J. Stevanovic, Y. Xie, J. Joseph, V. Maslak, C. M. Hadad and K. D. Glusac, *J. Phys. Chem. A*, 2016, **120**, 7294–7300.
- 93 V. Sichula, P. Kucheryavy, R. Khatmullin, Y. Hu, E. Mirzakulova, S. Vyas, S. F. Manzer, C. M. Hadad and K. D. Glusac, *J. Phys. Chem. A*, 2010, **114**, 12138–12147.
- 94 E. M. Kober, B. P. Sullivan and T. J. Meyer, *Inorg. Chem.*, 1984, **23**, 2098–2104.
- 95 D. Jacquemin, E. A. Perpete, G. E. Scuseria, I. Ciofini and C. Adamo, *J. Chem. Theory Comput.*, 2008, **4**, 123–135.
- 96 P. Muller and K. Brettel, *Photochem. Photobiol. Sci.*, 2012, **11**, 632–636.
- 97 I. E. Pomestchenko and F. N. Castellano, *J. Phys. Chem. A*, 2004, **108**, 3485–3492.
- 98 H. M. Guo, M. L. Muro-Small, S. M. Ji, J. Z. Zhao and F. N. Castellano, *Inorg. Chem.*, 2010, **49**, 6802–6804.
- 99 H. M. Guo, T. Kottke, P. Hegemann and B. Dick, *Biophys. J.*, 2005, **89**, 402–412.
- 100 J. Heberle, T. Kottke, B. Dick and P. Hegemann, *Biophys. J.*, 2002, **82**, 517A.
- 101 T. Kottke, B. Dick, R. Fedorov, I. Schlichting, R. Deutzmann and P. Hegemann, *Biochemistry*, 2003, **42**, 9854–9862.
- 102 T. Kottke, J. Heberle, D. Hehn, B. Dick and P. Hegemann, *Biophys. J.*, 2003, **84**, 1192–1201.
- 103 U. Megerle, M. Wenninger, R.-J. Kutta, R. Lechner, B. Koenig, B. Dick and E. Riedle, *Phys. Chem. Chem. Phys.*, 2011, **13**, 8869–8880.